

This item is the archived peer-reviewed author-version of:

Simple dispersion estimate for single-section quantum-dash and quantum-dot mode-locked laser diodes

Reference:

O Duill Sean P., Murdoch Stuart G., Watts Regan Trevor, Rosales Ricardo, Ramdane Abderrahim, Landais Pascal, Barry Liam P.- Simple dispersion estimate for single-section quantum-dash and quantum-dot mode-locked laser diodes

Optics letters / Optical Society of America - ISSN 0146-9592 - 41:24(2016), p. 5676-5679

Full text (Publisher's DOI): <http://dx.doi.org/doi:10.1364/OL.41.005676>

To cite this reference: <http://hdl.handle.net/10067/1402010151162165141>

Simple dispersion estimate for single-section quantum-dash and quantum-dot modelocked laser diodes

SEAN P. O DUILL,^{1,*} STUART G. MURDOCH,² REGAN T. WATTS,³ RICARDO ROSALES,⁴ ABDERRAHIM RAMDANE,⁵ PASCAL LANDAIS,¹ LIAM P. BARRY¹

¹The Radio and Optics Communications Laboratory, School of Electronic Engineering, Dublin City University, Dublin 9, Ireland

²Dodd-Walls Center for Photonic and Quantum Technologies, and Physics Department, University of Auckland, Private Bag 92019, Auckland, New Zealand

³Faculty of Integrated Technologies, Universiti Brunei Darussalam, Brunei Darussalam

⁴Institute of Solid State Physics, Technical University of Berlin, Hardenbergstr. 36, 10623 Berlin, Germany

⁵Laboratory for Photonics and Nanostructures, Centre National de la Recherche Scientifique, Paris 91460, France

*Corresponding author: sean.oduill@dcu.ie

Received XX Month XXXX; revised XX Month, XXXX; accepted XX Month XXXX; posted XX Month XXXX (Doc. ID XXXXX); published XX Month XXXX

The optical outputs of single-section quantum-dash and quantum-dot mode-locked lasers (MLL) are well-known to exhibit strong group velocity dispersion. Based on careful measurements of the spectral phase of the pulses from these MLLs, we confirm that the difference in group delay between the modes at either end of the MLL spectrum equals the cavity roundtrip time. This observation allows us to deduce an empirical formula relating the accumulated dispersion of the output pulse to the spectral extent and free-spectral-range of the MLL. We find excellent agreement with previously reported dispersion measurements of both quantum-dash and quantum-dot MLLs over a wide range of operating conditions. © 2016 Optical Society of America

OCIS codes: (140.4050) Mode-locked lasers; (140.5960) Semiconductor lasers; (140.3430) Laser theory; (260.2030) Dispersion; (320.2250) Femtosecond phenomena.

<http://dx.doi.org/10.1364/OL.99.099999>

Single-section mode-locked lasers (MLL) are a class of semiconductor MLL whereby a simple Fabry-Pérot laser supports multiple longitudinal lasing modes, with all of the modes mutually phase-locked. These MLLs contain neither an external locking mechanism, nor intracavity saturable absorber [1-8]. The mechanism by which these lasers modelock is often postulated to be four-wave mixing [2,8]. Single-section laser mode-locking phenomena have been observed and documented for bulk [1,2], quantum-well [5], quantum-dash [3,4], and quantum-dot [6,7]

devices. Whilst modelocked, these single-section devices exhibit strong group velocity dispersion and the temporal pulsations are not immediately visible [1, 7, 9-11]. The acquired dispersion is found to be normal such that short femtosecond pulses can be recovered simply by compensating with the correct amount of anomalous dispersion. For devices operating around 1.5 μm this can be achieved using an appropriate length of standard single mode fiber. At other wavelengths specialty dispersion-engineered fibers are needed. The preponderance of carefully obtained group velocity dispersion measurements of these MLLs have been performed for devices based on quantum-dash and quantum-dot materials, thus we restrict our study to just these devices. Measurements of the phase of the spectral modes of quantum-dash MLLs with a wide range of different free spectral ranges (FSR) and operating currents have been presented in Refs. [9-11]. These MLLs show extraordinarily large group velocity dispersions ranging from +1.33 to +3.08 ps^2 for pulses emanating from devices with sub-mm length. Thus, lengths of fiber of the order of tens or hundreds of meters are needed to restore the femtosecond pulsations [1, 9-11, 13].

In Ref. [7] it was first reported that the output of single-section quantum-dot MLLs were highly-chirped elongated pulses, and that the magnitude of the group delay difference between the modes at either end of the MLL spectrum was approximately equal to the cavity round trip time. In this Letter we present data that suggests that this observation is a general property of all single-section quantum-dash and quantum-dot MLLs. Using this knowledge, we derive a simple expression for the group velocity dispersion of the MLL in terms of the laser's spectral width and free-spectral-range

(FSR). Both of these parameters can be simply obtained from a measurement of the optical spectrum of the laser; hence a quick estimate for the dispersion would inform the length of fiber needed to compress the pulse. We present group velocity dispersion calculations in detail for two different single-section quantum-dash MLLs with FSRs of 23 GHz and 48 GHz for a wide range of bias currents. We find excellent agreement between the calculated group velocity dispersion using our simple equation and the measured value using an independent stepped heterodyne technique [12]. We also find that the decrease in group velocity dispersion observed with increasing device current occurs only because the spectral width of the MLL field increases with increasing bias current while the group delay difference between the modes at the frequency-extrema of the spectrum remains fixed. The formula also shows excellent agreement with our previous results that have been reported in the literature for a device with an FSR of 39.8 GHz FSR [10]

The measured group velocity dispersion of two quantum-dash MLLs with lengths of 1820 μm and 890 μm (corresponding to FSRs of 23 GHz and 48 GHz respectively) for five different bias currents have been presented in [9]. The measurement technique used was the stepped-heterodyne technique that is fully outlined in [12]. The working principle is that a tunable local oscillator laser is set to a frequency located close to a mode of the MLL spectrum. The resulting beat-notes are then recorded on a real-time oscilloscope. Repeating this measurement for all modes allows the full reconstruction of the amplitude and phase of the optical spectrum [12]. The measured optical spectra of the two MLLs at each bias current are reproduced in Fig. 1. It is clear that the width of the spectral envelope of the MLL increases with increasing bias current, with the spectral envelope reaching a maximum of 2.2 THz for both devices at 400 mA. The reason for the increase in spectral width with increasing bias current is due to the unusually large nonlinear gain-compression typical of a quantum-dash medium [8]. As the MLL power increases, the population inversion must increase in order to maintain the unity roundtrip gain criterion. The increase in population inversion means that carriers are excited to higher energy levels within the dashes and hence more modes attain sufficient gain to participate in the lasing process. In this work, we define the spectral width of the MLL field envelope Δf_{env} as the 10 dB bandwidth of the optical spectrum as this gives us the best measure of the spectral extent of the laser. The standard 3 dB definition cannot cope with the typical variations in mode power found across the lasing spectrum of these devices (see e.g. Fig. 1). Estimates for Δf_{env} are explicitly indicated for each spectrum shown in Fig. 1. The phase of each of the modes is retrieved by the stepped-heterodyne technique and the phases for each spectra are reproduced in Fig. 2 [9]. The spectral phase displays a distinct quadratic relationship and can be related to the group velocity dispersion by:

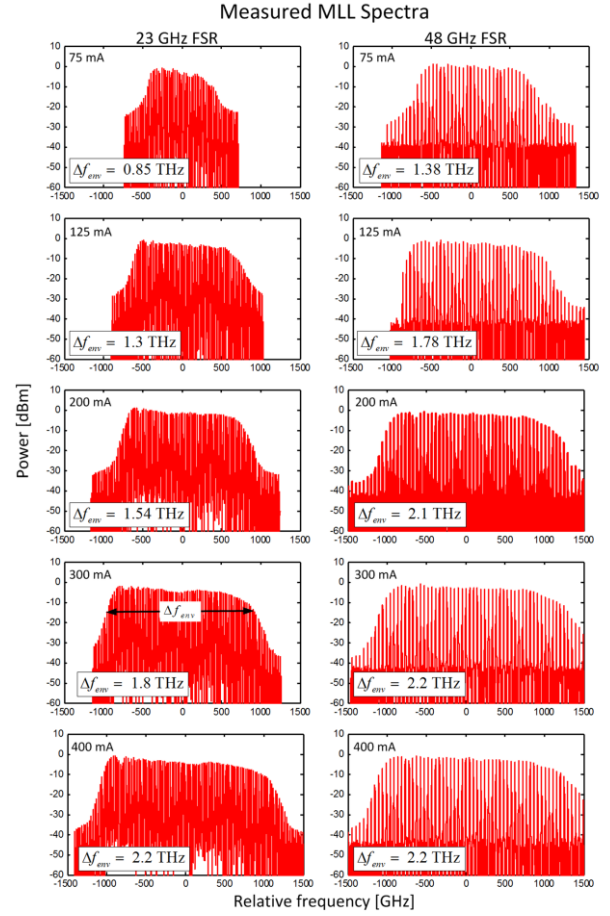


Fig. 1 Measured MLL spectra for the devices with FSRs of 23 GHz and 48 GHz. The curves were all measured using an optical spectrum analyzer. The definition of the spectral width of the MLL field envelope Δf_{env} is illustrated. The value for Δf_{env} is indicated on each spectral plot.

$$\phi_n = \frac{1}{2} B (2\pi [f_n - f_0])^2 \quad (1)$$

where B is the group velocity dispersion, f_n is the frequency of the n^{th} mode, and f_0 is the central frequency of the MLL. B is extracted for each operating current by fitting each quadratic curve in Fig. 2 to a parabola given by (1). Using the standard relationship between phase and group delay, the delay experienced by the n^{th} mode is given by:

$$\Delta\tau_n = - \left. \frac{1}{2\pi} \frac{d\phi}{df} \right|_{f=f_n} \quad (2)$$

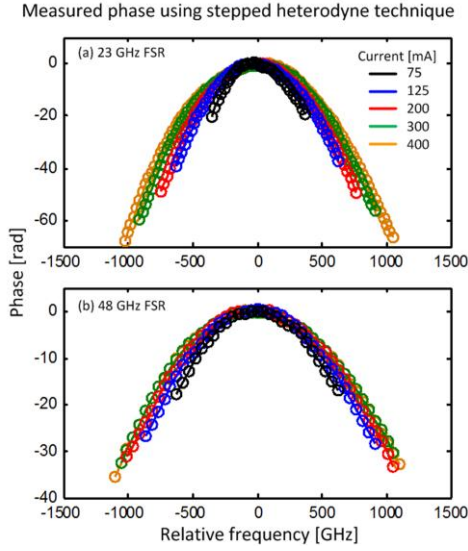


Fig. 2 Measured spectral phase using the stepped-heterodyne technique for (a) the 3 GHz FSR device and (b) the 48 GHz FSR device. Note that each curve is well approximated by a parabola. The MLL bias current is used as parameter.

To obtain our empirical relation, we set the difference in group delays experienced by the two modes at the frequency-extrema of the MLL spectrum to the cavity round trip time:

$$\Delta\tau_{env} = B(2\pi\Delta f_{env}) = \Delta f_{FSR}^{-1} \quad (3)$$

Where Δf_{env} is the 10 dB spectral width of the MLL field, and Δf_{FSR} is the FSR. Using this relation a simple expression for B appears as:

$$|B| = (2\pi\Delta f_{env}\Delta f_{FSR})^{-1} \quad (4)$$

Note that B is related to positive-valued quantities measurable using standard optical spectrum analyzers, thus this technique cannot distinguish between normal and anomalous dispersions. Typically pulses from MLLs exhibit normal dispersion, and hence dispersion compensation is achieved by passing the MLL output through an appropriate length of anomalous dispersion optical fiber [9-11, 13].

For each of the MLL operating bias currents in Fig. 1 we estimate Δf_{env} and Δf_{FSR} from the measured optical spectrum. This single measurement is all that is required to calculate B using Eqn. (4). The calculated values for B given by Eqn. (4), along with the independently measured values for B obtained from Fig. 2, are plotted in Fig. 3. There is remarkable agreement between the measured and calculated values for both devices at all operating bias currents we test. The longer 23 GHz device can accommodate approximately twice the pulse broadening of the 48 GHz device, and because of this, the group velocity dispersion values of the 23 GHz device are approximately double that of the 48 GHz device. When operating the MLLs at low bias currents of 75 mA, the

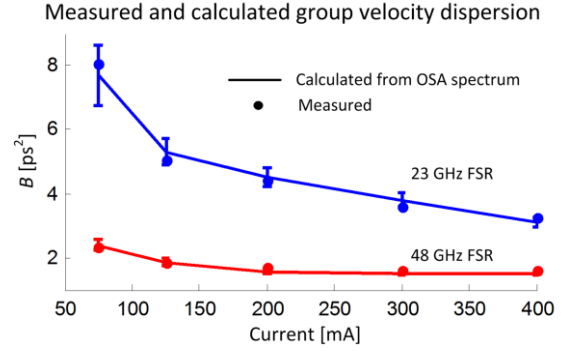


Fig. 3 Measured and calculated group velocity dispersion from two different quantum dash MLLs with FSRs of 23 and 48 GHz. The relation in Eq.-(4) holds for the two different FSR. The decrease in B with increasing current is attributed to the increasing spectral range of the MLL. The error bars show the range of B when estimating the MLL spectral width with an accuracy of 0.1 THz.

spectral width is much smaller than when operating with 400 mA; hence the larger values of B in this case.

We perform a standard error analysis. The relative variation of the FSR over the entire operational range of bias currents is at most 0.1% of the FSR [14], whereas the estimate for the error in Δf_{env} is 0.1 THz with relative errors ranging from 4.5% to 12%. We use the uncertainty in estimating Δf_{env} to calculate the error bars shown in Fig. 3. All of the calculated values for B fall within the error bars and the magnitude of the error bars decreases as the relative error in estimating Δf_{env} decreases.

Additional measured values of the group velocity dispersion of a 39.8 GHz FSR quantum dash MLL using the stepped heterodyne method were also reported in [10]. That device was operated at three different bias currents of 140 mA, 240 mA, and 340 mA, and by examining the spectra in [10] we can estimate Δf_{env} for each bias current. The results for the estimated group velocity dispersion are displayed in Table 1 and also show an excellent agreement between the measured values that are presented alongside. This further underscores the utility of the simple relation in (4).

We now estimate for the group velocity dispersion for a single-section quantum *dot* MLL with FSR of 4.6 GHz in [7]. The group velocity dispersion was measured by optically filtering parts of the MLL spectrum and then calculating the delay of the sinusoidal beat term using an oscilloscope; the group delay along the MLL spectrum was recorded by moving the central wavelength of the optical bandpass filter over the entire MLL spectrum [7] and noting the delay of the beat term. As noted in [7, Fig. 9(b)], the maximum difference in group delay is almost equal to the cavity roundtrip time. The spectral extent is estimated to range from 1527.5 nm to 1537 nm by inspection of [7, Fig. 9(b)]. The optical spectrum (without filtering) is shown in [7, Fig. 7(a)], we estimate that the 10 dB spectral extent of the spectrum ranges from 1527.5 nm to 1536.5 nm which is close to that measured from a direct measurement of the group delay. The estimated Δf_{env} from the optical spectrum gives a value of 1.152 THz; using (4) we calculate

Table 1 Dispersion results for the quantum dash device measured in [10].

Bias current (mA)	Δf_{env} [THz]	B Measured [10] [ps ²]	B Calculated [ps ²]
140	1.6	2.58	2.49
240	1.8	2.26	2.22
340	1.9	2.14	2.1

Table 2 Dispersion estimation for a quantum dot MLL [7].

Estimated Δf_{env} [THz]	Δf_{FSR} [GHz]	B Calculated [ps ²]
1.152	4.6	30.03

the group velocity dispersion to be 30.03 ps². The group velocity dispersion is large only because of the small spectral width and small Δf_{FSR} of 4.6 GHz. due to the long device length of 9 mm. The results for the quantum dot MLL are tabulated in Table 2.

In this letter we have examined the extraordinarily large group velocity dispersion of single-section MLLs and find that the group delay difference between the modes at the two extrema of the lasing spectrum is set by the MLL cavity round trip time. This allows us to present a simple formula that relates the GVD of a MLL to its spectral width and FSR. MLLs from quantum-dash and quantum-dot materials exhibit emission spectra with a sharp spectral cutoff thus facilitating the estimation of their spectral widths. The results in [7] showed that the difference in group delay of single section quantum dot devices equals the cavity round trip time; here we independently confirm that the relationship also holds of single section quantum dash MLLs. Moreover, the MLLs used here were independently fabricated, the dispersion/group delay measurements were performed using a different technique; and therefore we conclude that a hallmark of mode-locking within a single section quantum-dash or quantum-dot MLL is that the maximum group delay difference experienced by the modes equals the cavity round trip time. These observations present an interesting time-domain picture of the output of the device: as the output of the laser possess an almost purely linear normal GVD, and as the magnitude of the pulse broadening is equal to one roundtrip time, therefore the output light field can be considered as an approximately CW signal with an instantaneous frequency that sweeps continuously from the lowest to highest frequency of the optical spectrum with a period of one cavity roundtrip time [7]. The results and confirmation presented here of the characteristics of single-section MLLs should help lead to a full generalized theory to explain the operation of these devices [8]. It should be noted that no peculiarity of the underlying quantum-dash and dot material was invoked in deriving our formula with the only laser parameter defining the pulse broadening being the length of the MLL itself. We cannot verify the relation in (4) for MLLs made from quantum wells and bulk material because of the lack of sufficiently high quality measurements. Nonetheless, our results highlight an

important phenomenon of single-section MLLs and indicate a direction for further studies on the pulse broadening of single section MLLs.

Acknowledgement: We are grateful to the anonymous reviewers for their helpful suggestions, and especially for bringing Ref. [7] to our attention.

Funding. Science Foundation Ireland (SFI) (12/RC/1776, 10/CE/11853 and 14/IFB/2076), EU FP7 “BIG PIPES”.

References

1. K. Sato, IEEE J. Sel. Top. Quantum Electron. 9, No. 5, 1288, (2003).
2. J. Renaudier, G.-H. Duan, P. Landais, and P. Gallion, IEEE J. Quantum Electron. 43, No. 2, pp. 147-156, (2007).
3. G. H. Duan, A. Shen, A. Akrouf, F. Van Dijk, F. Lelarge; F. Pommereau, O. LeGouezigou, J.-G. Provost, H. Gariah, F. Blache, F. Mallecot, K. Merghem, A. Martinez, and A. Ramdane, Bell Labs Tech J. 14, No. 3, 63, (2009).
4. R. Rosales, K. Merghem, A. Martinez, A. Akrouf, J.-P. Tournenc, A. Accard, F. Lelarge, and A. Ramdane, IEEE J. Sel. Top. Quantum Electron. 17, No. 5, 1292, (2011).
5. C. Calò, V. Vujicic, R. Watts, C. Browning, K. Merghem, V. Panapakkam, F. Lelarge, A. Martinez, B.-E. Benkelfat, A. Ramdane, and L. P. Barry, OSA Optics Expr. 23, No. 20, pp. 26442-26449, (2015).
6. R. Rosales, K. Merghem, C. Calo, G. Bouwmans, I. Krestnikov, A. Martinez, and A. Ramdane, Appl. Phys. Lett. 101, 221113, (2012).
7. M. J. R. Heck, E. A. J. M. Bente, B. Smalbrugge, Y.-S. Oei, M. K. Smit, S. Anantathanasarn, and R. Nötzel, OSA Opt. Exp. 15, No. 25, pp. 16292-16301, (2007).
8. M. Gioannini, P. Bardella, and I. Montrosset, IEEE J. Sel. Topics in Quantum Electron. 21, No. 6, Article # 1900811, (2015).
9. R. Rosales, S. G. Murdoch, R.T. Watts, K. Merghem, A. Martinez, F. Lelarge, A. Accard, L. P. Barry, and A. Ramdane, Opt. Exp. 20, No. 8, 8649, (2012).
10. S. G. Murdoch, R. T. Watts, Y. Q. Xu, R. Maldonado-Basilio, J. Parra-Cetina, S. Latkowski, P. Landais, and L. P. Barry, Opt. Expr. 19, No. 14, 13628, (2011).
11. R. T. Watts, R. Rosales, S. G. Murdoch, F. Lelarge, A. Ramdane, and L. P. Barry, in Proc. of CLEO'12, Paper number CM1L.5, San Jose, (2012).
12. D. A. Reid, S. G. Murdoch, and L. P. Barry, Opt. Express 18(19), 19724–19731 (2010).
13. S. Latkowski, R. Maldonado-Basilio and P. Landais, Opt. Expr. 17, No. 21, 19166, (2009).
14. J. Müller, J. Hauck, B. Shen, S. Romero-García, E. Islamova, S. S. Azadeh, S. Joshi, N. Chimot, A. Moscoso-Mártir, F. Merget, F. Lelarge, and J. Witzens, Adv. Opt. Technol. 4, No.2, 119, (2015).

References

1. K. Sato, "Optical Pulse Generation Using Fabry-Pérot Lasers Under Continuous-Wave Operation," *IEEE J. Sel. Top. Quantum Electron.* 9, No. 5, 1288, (2003).
2. J. Renaudier, G.-H. Duan, P. Landais, and P. Gallion, "Phase Correlation and Linewidth Reduction of 40 GHz Self-Pulsation in Distributed Bragg Reflector Semiconductor Lasers," *IEEE J. Quantum Electron.* 43, No. 2, pp. 147 -156, (2007).
3. G. H. Duan, A. Shen, A. Akrouf, F. Van Dijk, F. Lelarge, F. Pommereau, O. LeGouezigou, J.-G. Provost, H. Gariah, F. Blache, F. Mallecot, K. Merghem, A. Martinez, and A. Ramdane, "High performance InP-based quantum dash semiconductor mode-locked lasers for optical communications," *Bell Labs Tech J.* 14, No. 3, 63, (2009).
4. R. Rosales, K. Merghem, A. Martinez, A. Akrouf, J.-P. Tourrenc, A. Accard, F. Lelarge, and A. Ramdane, "InAs/InP Quantum-Dot Passively Mode-Locked Lasers for 1.55- μ m Applications," *IEEE J. Sel. Top. Quantum Electron.* 17, No. 5, 1292, (2011).
5. C. Calò, V. Vujicic, R. Watts, C. Browning, K. Merghem, V. Panapakkam, F. Lelarge, A. Martinez, B.-E. Benkelfat, A. Ramdane, and L. P. Barry, "Single-section quantum well mode-locked laser for 400 Gb/s SSB-OFDM transmission," *OSA Optics Expr.* 23, No. 20, pp. 26442-26449, (2015).
6. R. Rosales, K. Merghem, C. Calò, G. Bouwmans, I. Krestnikov, A. Martinez, and A. Ramdane, "Optical pulse generation in single section InAs/GaAs quantum dot edge emitting lasers under continuous wave operation," *Appl. Phys. Lett.* 101, 221113, (2012).
7. M. J. R. Heck, E. A. J. M. Bente, B. Smalbrugge, Y.-S. Oei, M. K. Smit, S. Anantathanasarn, and R. Nötzel, "Observation of Q-switching and mode-locking in two-section InAs/InP (100) quantum dot lasers around 1.55 μ m," *OSA Opt. Exp.* 15, No. 25, pp. 16292-16301, (2007).
8. M. Gioannini, P. Bardella, and I. Montrosset, "Time-Domain Traveling-Wave Analysis of the Multimode Dynamics of Quantum Dot Fabry-Pérot Lasers," *IEEE J. Sel. Topics in Quantum Electron.* 21, No. 6, Article # 1900811, (2015).
9. R. Rosales, S. G. Murdoch, R.T. Watts, K. Merghem, A. Martinez, F. Lelarge, A. Accard, L. P. Barry, and A. Ramdane, "High performance mode locking characteristics of single section quantum dash lasers," *Opt. Exp.* 20, No. 8, 8649, (2012).
10. S. G. Murdoch, R. T. Watts, Y. Q. Xu, R. Maldonado-Basilio, J. Parra-Cetina, S. Latkowski, P. Landais, and L. P. Barry, "Spectral amplitude and phase measurement of a 40 GHz free-running quantum-dash modelocked laser diode," *Opt. Expr.* 19, No. 14, 13628, (2011).
11. R. T. Watts, R. Rosales, S. G. Murdoch, F. Lelarge, A. Ramdane, and L. P. Barry, "QDash semiconductor mode-locked lasers as compact subchannel comb for optical OFDM superchannel systems," in *Proc. of CLEO'12*, Paper number CM1L.5, San Jose, (2012).
12. D. A. Reid, S. G. Murdoch, and L. P. Barry, "Stepped-heterodyne optical complex spectrum analyzer," *Opt. Express* 18(19), 19724-19731 (2010).
13. S. Latkowski, R. Maldonado-Basilio and P. Landais, "Sub-picosecond pulse generation by 40-GHz passively mode-locked quantum-dash 1-mm-long Fabry-Perot laser diode," *Opt. Expr.* 17, No. 21, 19166, (2009).
14. J. Müller, J. Hauck, B. Shen, S. Romero-García, E. Islamova, S. S. Azadeh, S. Joshi, N. Chimot, A. Moscoso-Mártir, F. Merget, F. Lelarge, and J. Witzens, "Silicon photonics WDM transmitter with single section semiconductor mode-locked laser," *Adv. Opt. Technol.* 4, No.2, 119, (2015).